Congresso de Métodos Numéricos em Engenharia
1-3 julho 2019, Guimarães, Portugal
Universidade do Minho

VALIDATION MODELS ON THE FIRE RESISTANCE OF COMPOSITE SLAB WITH STEEL DECK

Paulo Piloto[1]; Carlos Balsa[1]; Fernando Ribeiro[2]; Ronaldo Rigobello[2];

Lucas Santos[2]; Érica Kimura[2].

1: Instituto Politécnico de Bragança, Portugal.
e-mail: {ppiloto, balsa}@ipb.pt

2: Universidade Tecnológica Federal do Paraná, Brazil.
e-mail: f.freire12@gmail.com, rigobello@utfpr.edu.br, lucasobmep@outlook.com, ekimura@utfpr.edu.br

Keywords: Fire resistance, composite slab, steel deck, experimental tests, numerical validation

Abstract *The composite slab with steel decking is widely used in every type of buildings which require fire resistance, in accordance to regulations and standards. The fire rating of this type of elements is determined by standard fire tests, accounting for Load (R), Integrity (E) and Insulation (I). A literature review from different investigations regarding the fire behaviour of composite slabs with steel deck is presented. A specific number of experimental tests were selected for the validation with three-dimensional finite element models. The fire resistance of composite slabs with steel deck may also be compared with simple calculation methods available in standards, such as EN 1994-1-2. The perfect contact model used for numerical simulation present some discrepancies from the experimental results, which can be eliminated by the use of an air gap between the steel deck and the concrete part of the slab. Other parameters are also investigated regarding the thermal and the mechanical loading systems, towards the best fit approximation for temperature and displacement.*

1. INTRODUCTION

A composite slab consists of a concrete topping cast on the top of a steel deck. Concrete slabs with steel decks are slabs that use steel deck as a permanent formwork and reinforced concrete placed on the top. This fact represents one of the main advantages of this building solution, because it reduces the construction time, requires less concrete, providing slender slabs. The use of composite slabs in buildings has become very popular since 1980. The overall depth can vary between 100 to 170 mm. The thickness of the steel deck can vary from 0.7 to 1.2 or more and this part of the element is normally galvanized to increase durability [1]**.** The steel deck may be directly exposed to accidental fire conditions, reason why this composite element requires fire resistance, in accordance to regulations and standards. The fire rating of this type of element is determined by standard fire tests, accounting for Load bearing (R), Integrity (E) and Insulation (I).

Several studies have been conducted to evaluate the fire resistance of concrete slabs with steel deck. In 1983, The European Convention for Constructional Steelwork ECCS [2], published some design rules applied to the design of composite concrete slabs with a profiled steel deck, exposed to a standard fire [3]. This document also presents a resume of several experimental tests developed in different European testing laboratories. According to this document, the explicit fire design calculation for composite slabs is not required when the fire requirements are smaller or equal than 30 minutes. This rule should only be applied if the slab was safely designed to run at room temperature. For the other cases, simple calculation formulae were presented in a basis of conservative approximations for a safer design procedure. In this technical note, it is also assumed that if the insulation criterion is fulfilled, then the integrity criterion is also fulfilled. The technical note also identified the existence of the membrane effect when the composite slab is relatively well attached to the boundary of the building structure.

In 1990, Hamerlinck et al. [4] satisfactorily predicted the thermal and the mechanical behaviour of different slab geometries under fire conditions using a developed numerical model. Approximations were used for the thermal properties of the materials. This can partially justify the differences between the nodal temperatures obtained with the numerical simulations and experimental results. Approximation was also presented for the displacement behaviour of the tested slabs.

In 1999, Bailey et al. [5] presented the results of two experimental full-scale tests (complete building) and observed that the performance of the structure under fire differed from what was expected from fire codes. In addition, it was concluded that calculation rules were also conservative. Both tests demonstrated that the behaviour of the structural element was different from what was normally observed in standard small-scale fire tests.

In the same year, Abdel-Halim et al [6] published a paper with the main goal of providing relevant data about the behaviour of fire exposed composite slabs adopting a model fire test facility. For this purpose, one sample with and another without additional longitudinal reinforcement bars were subjected to the ISO standard fire in the University of Salford, UK. Thereupon, the research was focused on the investigation of the effect of additional bars on the fire resistance as well as on the comparison of the fire resistance of the specimens with respect to integrity and insulation. Conclusively, it was observed that the sample without additional bars presented a lower rate of temperature rise at the unexposed surface when compared to the reinforced sample and thus, a higher fire resistance in both insulation and integrity criteria.

An analysis of the heat transfer in composite slabs from the Cardington building testing facility was performed in 2001, by Lamont et al. [7]. Four fire tests were performed in different floors of the building. An adaptive heat transfer model was used to estimate the temperatures through the slab. The code was able to model the moisture evaporation from the pores of the concrete by assuming a phase change for temperature equal to 100ºC. The developed model presented satisfactory results for most of the tests.

In 2002, Lim et al. [8] developed six fire tests on two-way concrete slabs, comprising three reinforced concrete flat slabs and three composite steel-concrete slabs. The main objective was to investigate the behaviour of unrestrained simply supported slabs. The three flat slabs had different amounts of reinforcing in order to investigate its effect on controlling crack widths to insure integrity. The slabs were submitted to a live load and standard fire during three hours. All the slabs presented extensive surface cracking and loss of moisture. The

amount of concrete damage was related to the amount of reinforcement. The slabs supported the full duration of the tests without collapsing. The fire resistance of the slabs in the tests exceed the predictions of the code recommendations. The tests were able to demonstrate the effect of tensile membrane action during a fire, despite the significant loss of flexural strength.

More recently in 2017, Guo-Qiang Li et al. [9], performed four tests in composite slabs with steel decking, which were fire rated with 90 minutes according to Eurocode 4 provisions. The slabs were tested with different combinations of secondary beams, direction of the ribs and location of the rebars. The experiments revealed that the temperatures of the furnace were below the standard fire curve ISO 834. After 100 minutes of testing, the temperatures at the bottom of the slabs (above the steel deck) were approximately 100 °C below the furnace temperature. The temperature on the unexposed surface was less than 100 °C, for the same time duration. From the thermal insulation standpoint and using the simple formulae, the predicted fire resistance was 93 min, which means that for this particular condition, the simple calculation method is conservative. The fire rating was determined by the load bearing capacity of the element. Debonding was also observed in all experiments, which can justify the existence of a thermal resistance to the heat flux coming from the bottom.

Still in 2017, Jian Jiang et al. [10] from the National Institute of Standards and Technology (NIST) presented a numerical study based on detailed and reduced-order models of heat transfer in composite slabs. The main objective of this research was to develop a reduced-order modelling approach applicable for both thermal and structural analysis, in order to simplify the analysis of the structural behaviour under fire conditions. Solid elements were used for the concrete slab and shell elements for the steel deck. Both detailed and reduced-order models were validated against experimental tests and a parametric study using the detailed model was conducted to evaluate the effect of some parameters on temperature development such as thermal boundary conditions, thermal properties of materials and slab geometry. In addition, the specific heat of the concrete was modified to better estimate the heat input in the web, and thereafter an equation for the modification was suggested. In order to consider the effects of the change in emissivity of the galvanized steel deck due to the melting of the zinc layer, a novel method to calculate the temperature-dependent emissivity was proposed. Generally speaking, it was observed that satisfactory results did not require a great refinement of the finite element mesh and temperatures at the unexposed side were mainly affected by the thickness of the concrete topping. The results of the proposed model for emissivity showed better agreement with experimental results than those calculated from EN 1994-1-2.

In 2018, an investigation of the thermal performance of composite slabs under standard fire conditions was conducted by Prates [11]. The key objective of this study was to develop two-dimensional numerical models using the software MATLAB and ANSYS in order to evaluate the fire resistance of different slab configurations according to the insulation criterion. Several numerical simulations were performed with the aim of analysing the effect of both concrete and steel decking thicknesses on the unexposed side temperature. Considering that the thermal behaviour is not influenced by the mechanical behaviour, experimental fire tests were conducted on two unloaded samples. Moreover, the results of numerical simulations were compared against results obtained with the experimental tests as well as the simplified method given in EN 1994-1-2 and NBR 14323. The fire resistance obtained from the numerical models was considerably smaller than those measured on the experimental tests and a

comparison between the numerical and simplified method results evidenced that the design rules seem to be unsafe. According to the numerical results, a new and better approach was proposed, considering a quadratic variation between the fire resistance and the effective thickness of the composite slab.
In this investigation, three different composite slabs with steel deck were numerically tested using the standard fire curve ISO 834 to evaluate the fire Insulation criterion (I) and one was selected to evaluate the load bearing fire criterion (R). Three-dimensional numerical simulations of thermal and load effects on composite slabs were performed using ANSYS software to investigate the thermal effects of standard fire exposure. In addition, an air gap with constant thickness is included between the steel and concrete in order to simulate the debonding effects. Effectively, previous investigations mention the separation between the steel deck and the concrete, which creates a thermal resistance in this interface.
The simulations are validated with experimental results published by three different investigations, namely Hamerlinck [1], Abdel-Halim et al. [6] and Lim et al. [8].

2. FIRE RESISTANCE CRITERIA

Composite slabs need to meet fire-safety requirements according to building codes. The fire requirements are normally specified by fire rating periods of 30, 60, 90 min or more. The fire rating of this type of building elements is normally made using standard fire tests [12, 13], and should consider the criteria for Integrity (E), Insulation (I) and Load Bearing (R). Usually, these tests are expensive and time-consuming. As a workaround, the fire resistance can be evaluated by means of numerical simulations or by the use of simple calculation methods. The fire resistance of the composite slabs is always defined with respect to standard fire exposure from below. In this work, the fire resistance is investigated based on both insulation and load bearing criteria.

2.1. Integrity (E)

The integrity (E) is the ability to withstand fire in one side and the assessment shall be made on the basis of measuring cracks or openings in excess of given dimensions, or the ignition of a cotton pad, or sustained flaming on the unexposed side. The integrity (E) criterion is usually verified because the floor slab is cast in situ, being the joints adequately sealed. Any cracks which may occur in the concrete during fire exposure are unimportant because the steel profile will prevent the passage of flames or hot gases.

2.2 Insulation (I)

The insulation (I) is the ability to withstand fire in one side and the assessment shall be made on the basis of the average temperature rise on the unexposed face limited to 140 °C above the initial average temperature, or; made on the basis of the maximum temperature rise at any point limited to 180 °C above the initial average temperature.

2.3 Load bearing (R)

The load bearing resistance for flexural loaded elements (R) is the ability to support the loading during the test and the assessment shall be made on the basis of limiting vertical displacement D ($D=L^2/400d$ [mm]), or limiting rate of vertical displacement ($Dd/dt=L^2/9000d$ [mm/min]), being L the clear span of the testing specimen in millimetres and d is the distance

from the extreme fibre of the cold design compression zone to the extreme fibre of the cold design tensile zone of the structural section, in millimetres.

3. EXPERIMENTAL TESTS

Three different types of trapezoidal composite slabs were selected to perform the numerical simulations. These ones correspond to experimentally tested slabs. The slab 1 was tested by Hamerlinck [1] (test number 2), slab 2 was tested by Abdel-Halim et al. [6] (test number 2), and slab 3 was tested by Lim et al. [8] (test number 4). All the composite slabs were exposed to the ISO 834 standard fire. The profiles of each of these slabs are shown, respectively, in Figures 1, 2 and 3.

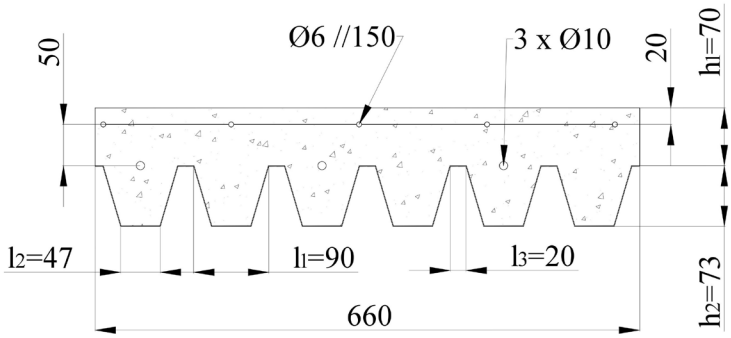

Figure 1. Profile of slab 1: dimensions in millimetres (Hamerlinck [1]).

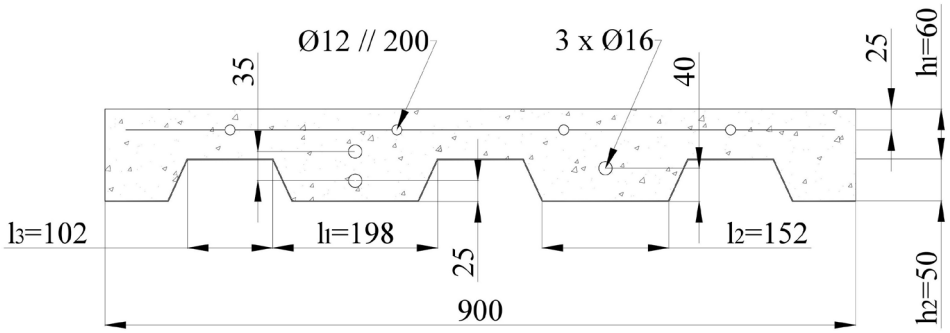

Figure 2. Profile of slab 2: dimensions in millimetres (Abdel-Halim et al. [6]).

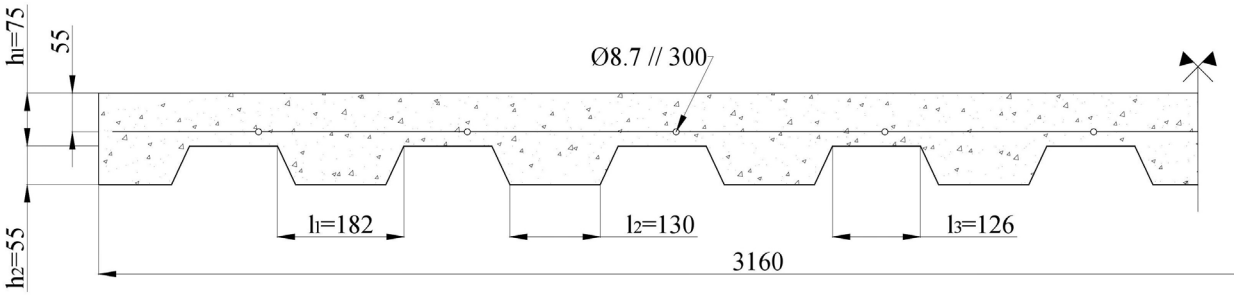

Figure 3. Profile of slab 3: dimensions in millimetres (Lim et al. [8]).

4. THERMAL ANALYSIS

In this section, the methodology used to model and numerically determine the thermal effects

on composite slabs subjected to standard fire conditions is outlined. In addition, the simplified calculation method of Eurocode 4 for determining the fire resistance of composite slabs with respect to the thermal insulation criterion is presented. The results are compared with the experimental results presented by Hamerlinck [1], Abdel-Halim et al. [6] and Lim et al. [8].

4.1. Heat transfer equation

The composite slab is meshed to solve a nonlinear transient thermal analysis, using 3D models from ANSYS. The finite element method requires the solution of equation (1) in the domain and equation (2) in the exposed side.

$$\nabla\left(\lambda_{(T)}.\nabla T\right) = \rho_{(T)}.Cp_{(T)}.\partial T/\partial t \tag{1}$$

$$\lambda_{(T)}.\nabla T.\vec{n} = \alpha_c\left(T_g - T\right) + \phi.\varepsilon_m.\varepsilon_f.\sigma.\left(T_g^4 - T^4\right) \tag{2}$$

In these equations: T represents the temperature of each material; $\rho_{(T)}$ is the specific mass; $Cp_{(T)}$ is the specific heat; $\lambda_{(T)}$ is the thermal conductivity; α_c is the convection coefficient. T_g represents the gas temperature of the fire compartment, using a standard fire ISO 834 applied to the bottom part of the slab; ϕ is the view factor; ε_m is the emissivity of each material; ε_f specifies the emissivity of the fire and σ represents the Stefan-Boltzmann constant.
The heat flow criterion was used for the convergence criterion, using a tolerance value of 0.001 and a minimum reference value of 10^{-6}.

4.2. Finite element model

The heat transfer equation is solved numerically by the Finite Element Method (FEM) using the ANSYS software. For a composite slab with trapezoidal steel deck, the respective 3D mesh is presented in Figure 4.

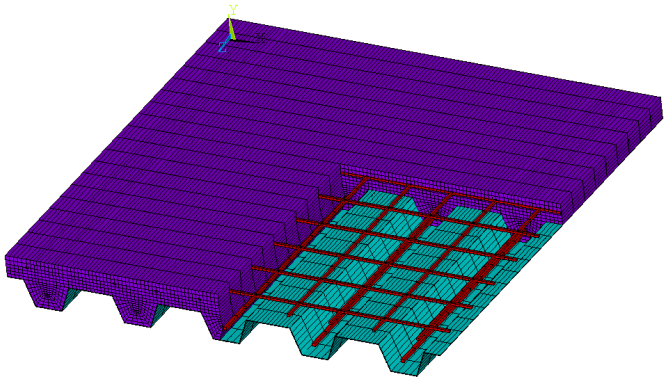

Figure 4. 3D finite element mesh with perfect contact.

A three-dimensional model of the slab is generated, being composed by subdomains corresponding to the different materials, namely the concrete topping, the steel deck, the steel rebars and the steel mesh. Additionally, in some simulations an air gap is included between the steel deck and the concrete. For each material, a specific 3D finite element is used, according to the geometry of the subdomain to be simulated.
Three different finite elements are used: SHELL131, SOLID70 and LINK33. The SHELL131 element has four nodes with up to 32 degrees of freedom (temperature) per

node, depending on the number of layers (one layer). This element presents linear interpolating functions in the plane of the element, using full Gauss integration method (2x2) and linear interpolating functions through the layer thickness utilizing three Gauss points. The shell element is used to model the steel deck of the composite slab. The SOLID70 element presents eight nodes with a single degree of freedom (temperature) at each node. Linear interpolating functions are used for this element and the full Gauss integration method is also applied (2x2x2). This finite element is used to model the concrete topping and, in some cases, the air gap. The LINK33 element has two nodes with a single degree of freedom (temperature) per node. This uniaxial element presents linear interpolating functions as well as exact interpolation. The LINK33 element is used to model the steel reinforcement, that is, the anti-crack mesh and the rebars.
The numerical solution of the partial differential equation (1) is nonlinear because the thermal properties (specific heat, density and conductivity) of the materials (concrete, steel and air) are temperature dependent. The exposed side is submitted to a heat flux by convection and radiation, see equation (2), using different view factors and a bulk temperature following the standard fire. The unexposed side is submitted to a convective heat flux (including the radiation heat flux), using a constant bulk temperature of 20ºC.

4.3. View factor

The view factor (ϕ) specified in the equation (2), quantifies the geometric relation between the surface emitting radiation and the receiving surface, that is dependent of the surfaces areas and orientations, as well as the distance between them. The view factor of the lower flange of the composite slab is given as ϕ_{low}= 1. The view factor of the web and upper flange of the steel deck are smaller than one, due to the obstruction caused by the ribs of the steel deck. These values can be calculated using Hottel´s crossed-string method [14]. This method is also incorporated in the EN 1994-1-2. The resulting equations for the upper flange (ϕ_{upper}) and web (ϕ_{web}) view factors are presented in equations (3) and (4). These equations allow the calculation of the view factors as functions of the parameters that describe the geometry of the slab, see Figures 1, 2 and 3. Figure 5 illustrates the components of a trapezoidal composite slab.

$$\phi_{upper} = \frac{ad + cb - ab - cd}{2ab} = \frac{\sqrt{h_2^2 + \left(l_3 + \frac{l_1 - l_2}{2}\right)^2} - \sqrt{h_2^2 + \left(\frac{l_1 - l_2}{2}\right)^2}}{l_3} \tag{3}$$

$$\phi_{web} = \frac{ac + cd - ad}{2ac} = \frac{\sqrt{h_2^2 + \left(\frac{l_1 - l_2}{2}\right)^2} + \left(l_3 + l_1 - l_2\right) - \sqrt{h_2^2 + \left(l_3 + \frac{l_1 - l_2}{2}\right)^2}}{2\sqrt{h_2^2 + \left(\frac{l_1 - l_2}{2}\right)^2}} \tag{4}$$

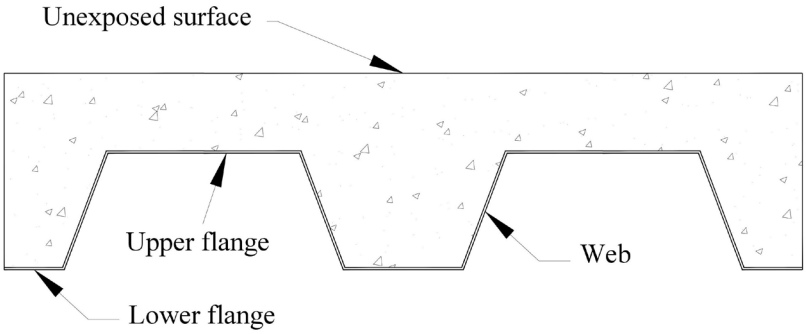

Figure 5. Schematic of the components of an arbitrary composite slab (adapted from [15]).

4.4. Thermal properties of materials

The thermal properties of the materials are temperature dependent and vary according to the standards used for composite slabs, steel structures and concrete structures [15, 16, 17]. The thermal properties of steel and concrete are depicted in Figure 6 and 7, respectively. The conductivity of steel decreases as long as the temperature increases and the specific heat has a strong variation due to the allotropic phase transformation. The density and the conductivity of concrete decrease as the temperature increase, and for the second, the upper limit was selected for the simulations. The specific heat of concrete presents a peak value related to 3% of moisture content of concrete weight.

Figure 8 depicts the thermal properties of air. These properties are also temperature dependent and were used to simulate the interface between the steel deck and the bottom surface of the concrete.

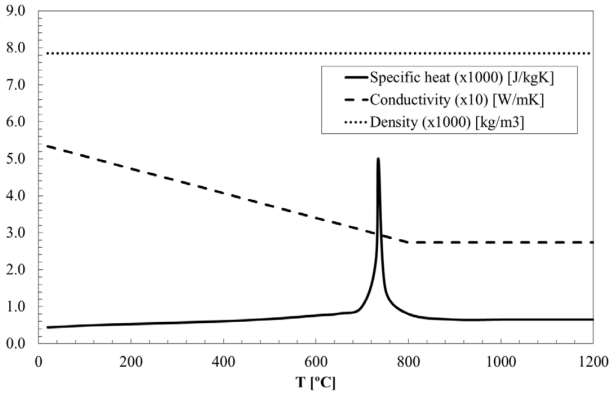

Figure 6. Thermal properties of carbon steel.

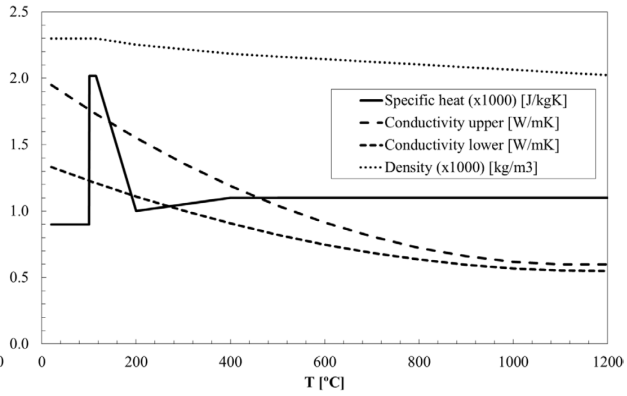

Figure 7. Thermal properties of concrete.

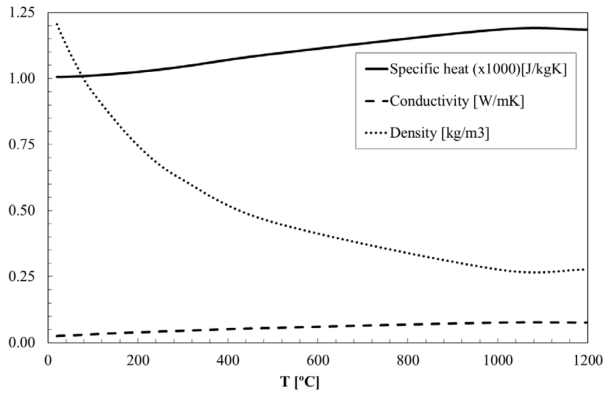

Figure 8. Thermal properties of air.

4.5. Boundary conditions

An initial condition for temperature is applied to all nodes (20ºC). The lower part of the deck is submitted to standard fire conditions, using a convection coefficient of 25 [W/m²K] and the emissivity of the fire equal to 1. The upper part of the slab is submitted to a convective coefficient of 9 [W/m²K] in order to include the radiation effect [18]. The main parameters of the boundary conditions are depicted in Figure 9.

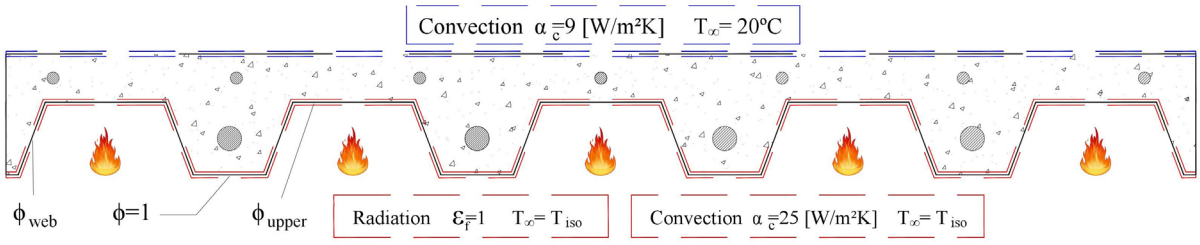

Figure 9. Definition of the slab geometry and representation of the boundary conditions.

4.6. Simplified calculation method of Eurocode 4

The Annex D of EN 1994-1-2 [15] presents a simplified method for the calculation of the fire resistance of unprotected composite slabs exposed to fire from below, when using the

standard fire curve ISO 834 [3]. The fire resistance (t_i) with respect to thermal insulation criterion should be determined according to the equation (5).

$$t_i = a_0 + a_1 \cdot h_1 + a_2 \cdot \phi_{upper} + a_3 \cdot \frac{A}{L_r} + a_4 \cdot \frac{1}{l_3} + a_5 \cdot \frac{A}{L_r} \cdot \frac{1}{l_3} \quad (5)$$

The rib geometry factor (A/L_r) of the slab should be determined as follows:

$$A/L_r = h_2 \cdot \left((l_1 + l_2)/2\right) \Big/ \left(l_2 + 2\sqrt{h_2^2 + \left((l_1 - l_2)/2\right)^2} \right) \quad (6)$$

In addition to the geometric parameters of the slab, the fire resistance also depends on partial factors (a_i). Table 1 presents these factors for normal weight concrete (NWC).

a_0 (min)	a_1 (min/mm)	a_2 (min)	a_3 (min/mm)	a_4 (mm min)	a_5 (min)
-28.8	1.55	-12.6	0.33	-735	48.0

Table 1. Coefficients for determination of the fire resistance for NWC (adapted from EN 1994-1-2 [15]).

4.7. Results

The Figures 10, 11 and 12 illustrate the temperature development (numerical and experimental) at different selected points as well as the average and maximum temperatures at the unexposed surface of the slab for the three validation models.

From the results of the slab 1, it can be concluded that the temperature development on the selected points is quite similar between the experimental (EXPT) and the perfect contact model (NUM 0) at the first minutes of heating. For temperatures over 100 °C, the model with the air gap (NUM 1 – 1 mm) present good approximation to the experimental results for point 2. However, for the points 1 and 3, the perfect contact model presents better agreement with measured temperatures at the last minutes of heating. For the unexposed surface, the maximum and average temperature curves are very close for all the models. Better agreement with the experimental results can be noticed using the model with the air gap.

For slab 2, it is noteworthy that the furnace temperature of the test is under the standard fire curve, which is used for the numerical simulations. For the model with the air gap (NUM 2 – 2 mm), the temperature development at points 1 and 3 presents better agreement with measured temperatures (EXPT). For point 2, a good agreement is observed between the perfect contact model (NUM 0) and experimental results until the first 44 minutes. After that, the air gap model better predicts the experimental result. For the unexposed side, big differences are observed between the results of the perfect contact and air gap models. Concerning the average temperature, a reasonable agreement with experimental results is obtained using the air gap model. For all measured temperatures, a slight plateau at about 100 °C should be highlighted, resulting in a delay in the rate of temperature increase due to the moisture content.

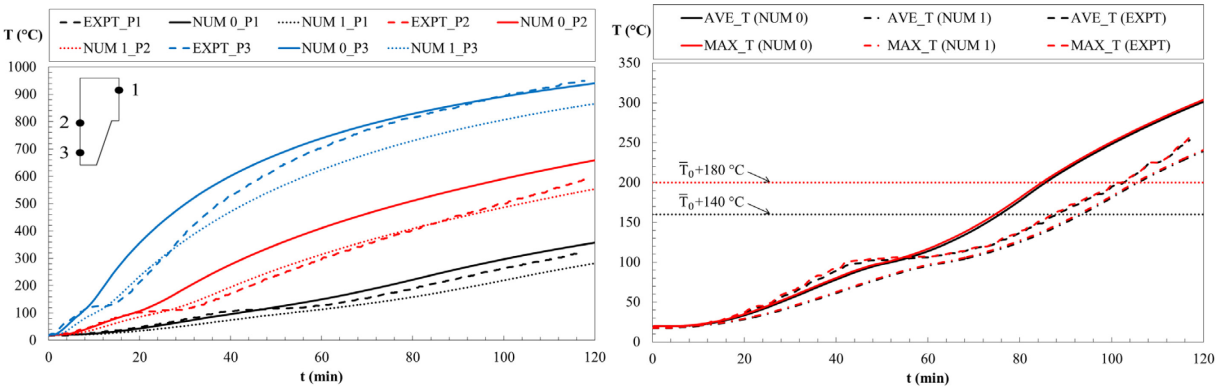

a) selected points. b) unexposed side.

Figure 10. Comparison between numerical and experimental results for slab 1. Point 1, 2 and 3 at distance 20, 74 and 123 mm from the top.

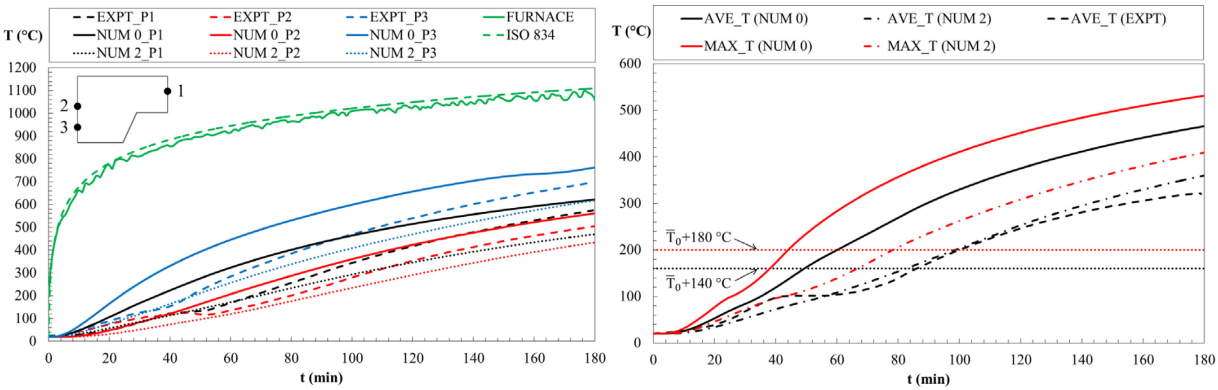

a) selected points. b) unexposed side.

Figure 11. Comparison between numerical and experimental results for slab 2. Point 1, 2 and 3 at distance 25, 50 and 85 mm from the top.

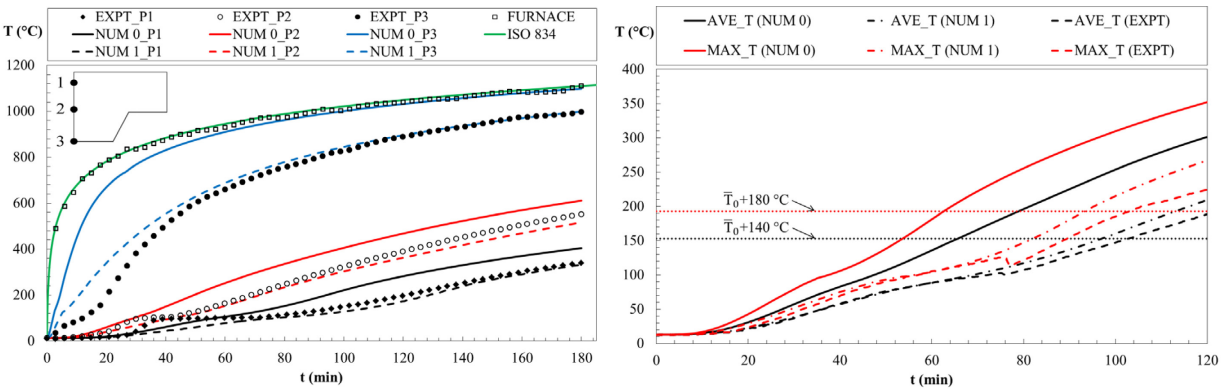

a) selected points. b) unexposed side.

Figure 12. Comparison between numerical and experimental results for slab 3. Point 1, 2 and 3 at distance 20, 70 and 130 mm from the top.

With respect to slab 3, a reasonable agreement is observed between the furnace temperature and the standard fire curve ISO 834. For the perfect contact model (NUM 0), a considerable difference between numerical and experimental results (EXPT) can be observed in the first stages of heating. On the other hand, regarding the air gap model (NUM 1 – 1 mm), a good

agreement is observed between numerical results and measured temperatures. For the results of the unexposed surface, concerning the air gap model, the accordance between the computed and measured temperatures is very good for both average and maximum temperatures until 76 minutes. After that, the differences are not so good, probably due to experimental deviations conditions, such as the furnace temperature, for example.
The following tables present the fire resistance (t_i – criterion 'I') with respect to both the average temperature rise (140 °C) and the maximum temperature rise (180 °C) at the unexposed side for each validation model.

	Model NUM 0	**Model NUM 1**	**EXPT result**	**EN 1994-1-2 result**
t_i Ave (min)	*75.6*	*93.5*	*88.2*	*106.5*
t_i Max (min)	84.8	105.1	102.1	

Table 2. Fire resistance according to thermal insulation criterion: experimental, numerical and analytical results for slab 1.

	Model NUM 0	**Model NUM 2**	**EXPT result**	**EN 1994-1-2 result**
t_i Ave (min)	49.4	82.6	*80.0*	*73.9*
t_i Max (min)	*44.1*	*78.3*	-	

Table 3. Fire resistance according to thermal insulation criterion: experimental, numerical and analytical results for slab 2.

	Model NUM 0	**Model NUM 1**	**EXPT result**	**EN 1994-1-2 result**
t_i Ave (min)	65.6	97.0	*102.7*	*95.8*
t_i Max (min)	*62.6*	*93.3*	103.0	

Table 4. Fire resistance according to thermal insulation criterion: experimental, numerical and analytical results for slab 3.

Concerning the slab 1, the results show that the air gap model slightly overestimated the fire resistance, with a relative error of 6%. The EN 1994-1-2 provisions overestimated the fire endurance, providing an unsafe result with a relative error of 20.7%.
For slab 2, a good agreement between the fire resistance obtained with the air gap model and experimental results is achieved (2.1% relative error). In addition, a good accordance is observed between EN 1994-1-2 calculations and experimental data, resulting in a relative error of 7.6%.
The results obtained with the air gap model underestimate the fire resistance for slab 3, with a relative error of 9.2%. Better approximation to experimental results is observed for the EN 1994-1-2 provisions, with a relative error of 6.7%.
More recently, Jian Jiang et al. [19] propose an improved algebraic formula for the calculation of the fire resistance (criterion I) that explicitly considers the effect of the moisture content and is applicable to an extended range of slab geometries. The proposed expression is developed based on simulations obtained from a validated finite element model.

5. MECHANICAL ANALYSIS

The mechanical simulation for the fire behaviour of the composite slabs is also analysed. The

model is validated with reference to the work developed by Hamerlinck [1]. The displacement and the rate of displacement is calculated, compared with the experimental results and compared with the criterion for fire rating given by EN 1363-1 [12].

5.1 Static equilibrium

The integral value of the surface force over any surface of an arbitrary volume element within the material must sum to zero in order to keep the static equilibrium. Here we assume the existence of an external load {F} (live and dead load) on material within the volume submitted to the stress field [σ]. The surface integral can be converted to a volume integral by the Gauss' divergence theorem. The final version of the equilibrium equation may be expressed in every cartesian coordinate, according to equation (7).

$$\nabla[\sigma]+\{F\}=\{0\} \tag{7}$$

The external load {F} is considered to be constant under fire conditions. The load bearing capacity was determined for room temperature, using expression (8) for sagging moment resistance and assuming the neutral axis to be located above the steel deck. $M_{p,Rd}$ represents the plastic bending resistance, $N_{p,pl}$ the plastic tensile force for the effective section of the plate, $N_{s,pl}$ the plastic tensile force for rebars, d_p represents the centroidal position for the plate measured from the top of the cross-section, x_{pl} represents the position for the plastic neutral axis measured from the top and d_s represents the position of the rebars measured from the top.

$$M_{p,Rd}=N_{p,pl}\times\left(d_p-\frac{x_{pl}}{2}\right)+N_{s,pl}\times\left(d_s-\frac{x_{pl}}{2}\right) \tag{8}$$

5.2 Finite element model

The finite element model uses a full three-dimensional finite element mesh, by switching the thermal SOLID70, SHELL131 and LINK33 finite element to the equivalent mechanical finite element SOLID185, SHELL181 and LINK180. The composite slab model with trapezoidal steel deck, is made with steel deck profile PRINS PSV73, see Figures 1 and 13.

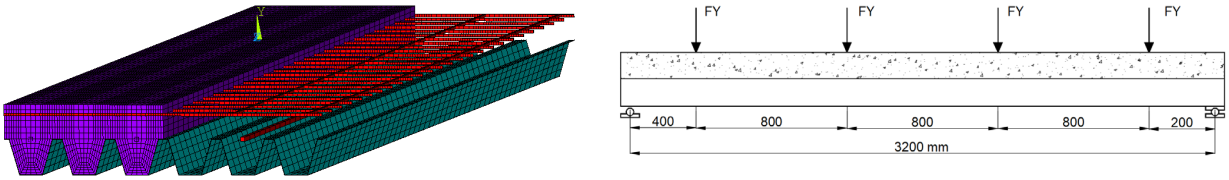

Figure 13. 3D finite element mesh (perfect contact) and physical model adapted from Hamerlinck test.

The mechanical load is distributed over 4 lines of nodal loads, with a spacing of 800 mm. This load represents the live load (used as parameter). The dead load is included by means of inertial effect (2800 N/m^2). The composite slab is considered to be simply supported (restraining the displacements in vertical and out-of-plane directions at the left support and restraining all displacements in the right support). The incremental solution, based on Newton Raphson method is used with a convergence criterion defined by force and moment, for a tolerance value of 0.001 and a minimum reference value of 1. The elastic-plastic analysis was

also used, considering the non-linear material properties and a non-linear geometric analysis. SOLID185 is a three-dimensional finite element defined by eight nodes, having three degrees of freedom at each node (3 translations). This element uses linear interpolation functions and full gauss integration. SHELL181 is a four-node element with six degrees of freedom at each node (3 translations and 3 rotations). This element also uses linear interpolating functions for in-plane with full integration scheme and linear interpolating functions in-thickness direction with 3 integration points. LINK180 is a unidirectional finite element with 2 nodes and 3 degrees of freedom at each node (translations). This element is superposed to the concrete nodes and uses 1 integration point.

5.3 Material properties

The mechanical properties of the materials are temperature dependent and vary according to the standards used for composite slabs [15], steel structures [16] and concrete structures [17]. Figures 14-16 present the stress-strain relation for all the materials. The thermal expansion for each material was also considered in the model, due to the existence of a very high temperature gradient through thickness. This gradient is responsible for the existence of thermal bowing, increasing the rotation of the cross-section.

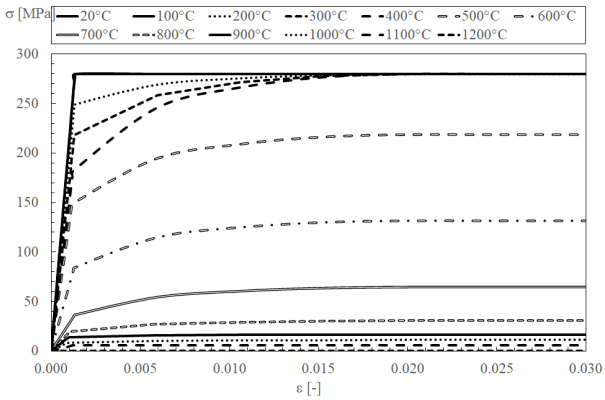

Figure 14. Mechanical properties of galvanized steel.

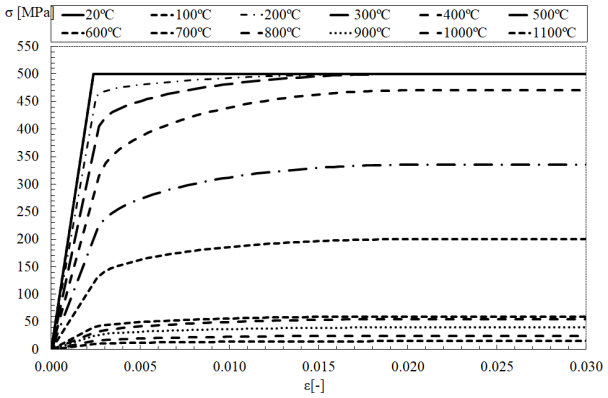

Figure 15. Mechanical properties of reinforcement.

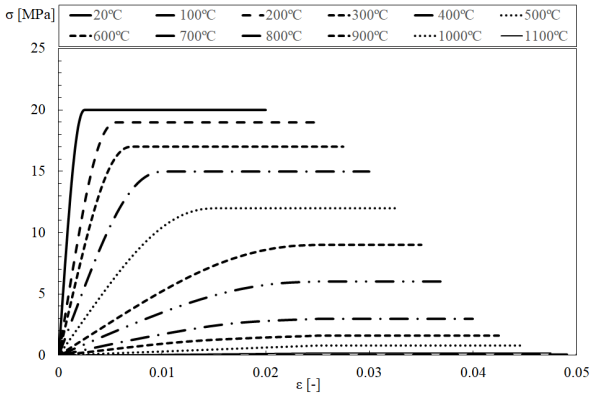

Figure 16. Mechanical properties of concrete.

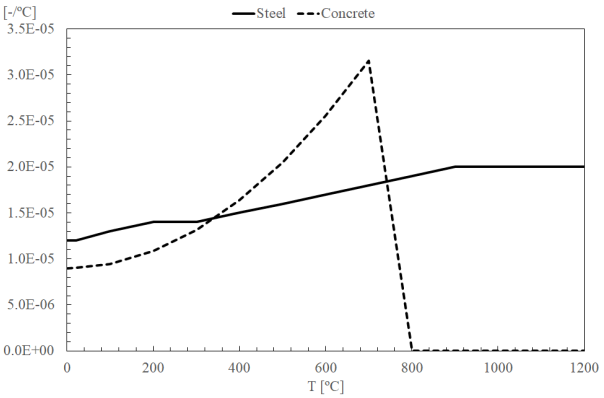

Figure 17. Coefficient for thermal expansion.

The change of thermal expansion with temperature, denoted as the coefficient of thermal expansion, is not constant, especially for concrete. Due to shrinkage, the expansion of

concrete stops at elevated temperatures (beyond 650 ºC). The expansion coefficient for steel has smaller variation with temperature. Changes in the microstructure explain the plateau between 750 and 800ºC.
All the material models were considered elastic, elliptic and perfect plastic.

5.4 Boundary conditions

The simply supported boundary condition was applied in the 3D mechanical model, considering the double support on the right extremity and the simple support on the left extremity. Four lines of nodal forces were applied in accordance to the experimental setup, see Figure 18. The dead load was calculated based on the volume and density of each material, using the inertial effect. The thermal effect introduces the incremental time effect, using different files with the temperature field for each time step.

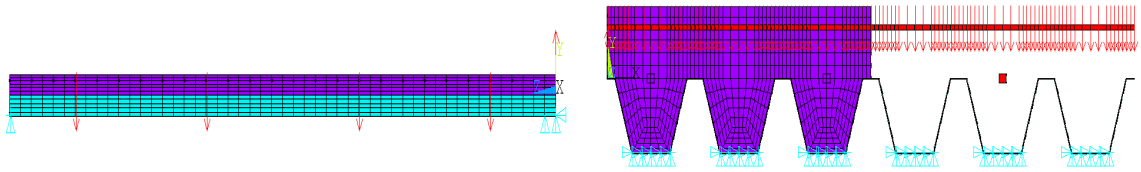

Figure 18. Boundary conditions for thermal and mechanical effects.

5.5 Results

The validation of the numerical model is based on the experimental results obtained by Hamerlinck [1]. In his test number 2, three vertical displacements were measured (D1, D2 and D3). The structure had a safety measure to protect the furnace. At the end of the test, the specimen made contact with the supporting beam, preventing their distortion into the furnace. D1 was selected to compare the numerical results. The time derivative dD1/dt was also considered for comparison, see Figure 19.

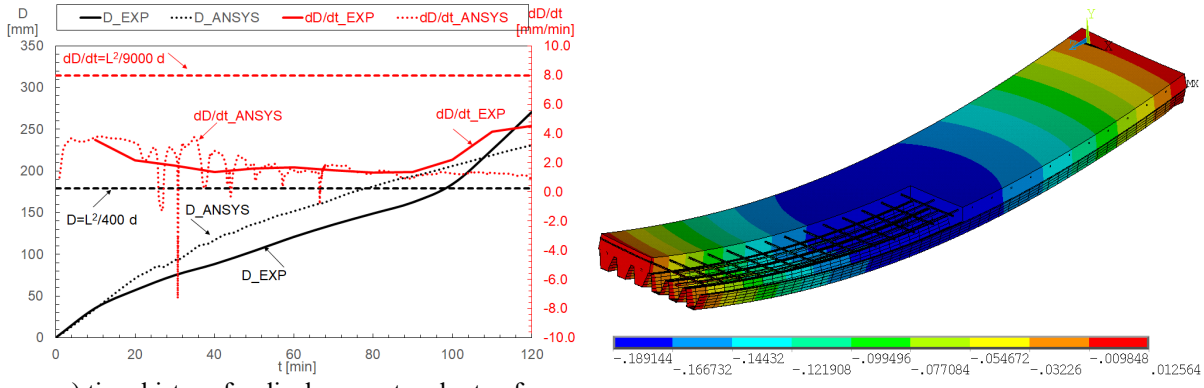

a) time history for displacement and rate of displacement.

b) deflection of the slab at the critical time.

Figure 19. Analysis of the composite slab with a live load of 2.7 kN/m^2.

The vertical displacement of the slab changes with time. The curvature of the slab starts increasing rapidly and deflections increase accordingly. In a second stage, the deflection rate decreases as thermal curvature increases less. Near the ultimate limit state, the deflection rate

increases again due to the plastic material behaviour. The rate of displacement is also depicted in Figure 19, being the numerical results very close to the experimental outcome. For the mechanical analyses, it should be highlighted that the thermal load was determined based on the perfect contact model between materials. That is, the effect of the air gap between the steel deck and concrete was not taken into consideration. These results in higher temperature values for the materials reflect on higher predicted values for the vertical displacement of the numerical results.

The fire resistance depends on the maximum displacement and rate of displacement. The first criterion was observed after 78 minutes of fire exposure (obtained from numerical simulation) in comparison with 97 minutes of fire resistance (obtained from experimental tests). The difference between both results can be explained by several factors, mainly by the temperature field in each time step. Other parameters are also reported and are related with several phenomena during the test (variation of the view factors, creation of the air gap effect between the steel deck and concrete, restrain effect in the supports, direction of the applied load during the test, among others).

A parametric analysis was developed, relating the amount of live load and the fire resistance. The load level was determined by the ratio of the total load (live and dead) by the plastic load at room temperature, proposed by the EN 1994-1-1 [20]. The fire resistance decreases with the load level, see Figure 20. The critical temperatures of the steel components were determined based on the fire resistance criteria. These values also decrease with the load level. The fire resistance for load bearing was always defined by the critical displacement value (D). The rate of displacement (dD/dt) never reached the critical value for load level values below 43%. For higher load levels, the critical displacement rate becomes important, but never anticipates the time for the critical displacement. The thermal gradient can be easily determined for each load level, being approximately equal to 700 ºC/123 mm in the vertical direction. This value seems to be independent of the load level.

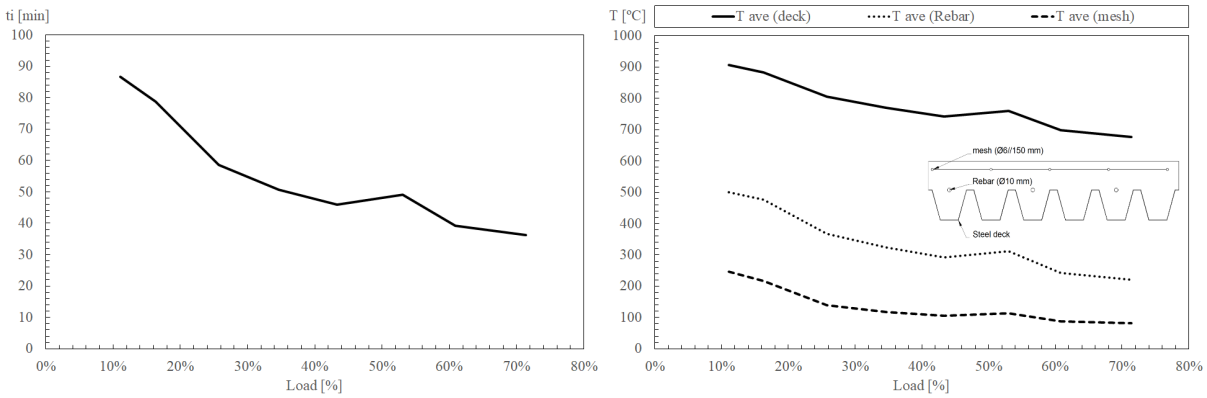

a) Fire resistance. b) Critical temperature.

Figure 20. Fire resistance and critical temperature for the steel components.

In practice, the rebars should be applied to composite slabs with steel deck, in cases when the required fire resistance time is higher than 30 minutes. When these elements are submitted to fire exposure, the contribution of the steel deck to the load bearing resistance decreases considerably, being part of this capacity transferred to the rebars.

6. CONCLUSIONS

This paper presented the description and the results obtained for the validation of the thermal and mechanical three-dimensional finite element models. The fire resistance with respect to thermal insulation (I) and load bearing (R) criteria was evaluated and compared to experimental results and to the results of simple calculation method. In order to simulate the effects of the debonding of the steel deck from concrete, an insulating layer (air gap) was introduced between the concrete and steel deck with a constant thickness.

Concerning the thermal model, for the experimental results of all the investigated slabs, a plateau at about 100 °C (due to moisture evaporation) should be highlighted, resulting in a delay in the rate of temperature increase. The numerical results do not present this pronounced plateau possibly because localized moisture concentrations may be higher than the moisture content introduced in the model. The moisture contents in slab 1, 2 and 3 were considered as 3.5%, 3% and 5.6%, respectively.

The fire resistance with respect to the thermal insulation criterion (I) was governed by the average temperature rise criterion for slab 1 and by the maximum temperature rise for slabs 2 and 3. The perfect contact model underestimates the fire resistance. In general, the results obtained with the air gap model presented better agreement with experimental results and satisfactorily simulates the debonding effect, reducing the temperature rise at the selected points and unexposed side as well.

The Eurocode 4 provisions for the fire resistance according to thermal insulation criterion (I) were generally on the safe side, with exception of slab 1.

The mechanical model underpredicts the fire resistance for load bearing condition. This is probably due to the difference between the temperature field used in the numerical model to load the composite slab (Model NUM 0) and the experimental temperature field.

A parametric analysis was developed to investigate the effect of the load level on the fire resistance of the slab 1. The fire resistance decreases with the load level. The critical temperature was determined in each simulation, for the steel components (steel deck, rebars and mesh). A higher critical temperature (on average) is predicted for the steel deck. The temperature gradient in the vertical direction is 6ºC/mm, being this value almost constant for every critical time, determined for each load level.

REFERENCES

[1] A. F. Hamerlinck, “The behaviour of fire-exposed composite steel/concrete slabs,” PhD thesis, Eindhoven University of Technology, 1991.

[2] ECCS - Committee T3 - Fire Safety of Steel Structures, “Calculation of the fire resistance of composite concrete slabs with profiled steel sheet exposed to the standard fire”, ECCS: Publication 32. ECCS, Committee T3 - Fire safety of steel structures, technical note, p. 48, 1983.

[3] International Organization for Standardization, “ISO 834-1: Fire Resistance Tests - Elements of Building Construction - Part 1: General Requirements.” International Organization for Standardization, Switzerland, p. 25, 1999.

[4] R. Hamerlinck and J. W. B. Stark, “A numerical model for fire-exposed composite steel / concrete slabs,” in 10th International Specialty Conference on Cold-Formed Steel Structures - International Specialty Conference on Cold-Formed Steel Structures. 5., 1990, pp. 115–130.

[5] C. G. Bailey, T. Lennon, and D. B. Moore, “The behaviour of full-scale steel-framed buildings subjected to compartment fires,” Struct. Eng., vol. 77, no. 8, pp. 15–21, 1999.
[6] M. A. H. Abdel-Halim, M. R. Hakmi, and D. C. O’Leary, “Fire resistance of composite floor slabs using a model fire test facility,” Eng. Struct., vol. 21, no. 2, pp. 176–182, 1999.
[7] S. Lamont, A. S. Usmani, and D. D. Drysdale, “Heat transfer analysis of the composite slab in the Cardington frame fire tests,” Fire Saf. J., vol. 36, no. 8, pp. 815–839, Nov. 2001.
[8] L. Lim and C. Wade, “Experimental Fire Tests of Two-Way Concrete Slabs - Fire Engineering Research Report 02/12,” Christchurch, New Zealand, 2002.
[9] G.-Q. Li, N. Zhang, and J. Jiang, “Experimental investigation on thermal and mechanical behaviour of composite floors exposed to standard fire,” Fire Saf. J., vol. 89, pp. 63–76, 2017.
[10] J. Jiang, J. A. Main, F. Sadek, and J. M. Weigand, “Numerical modeling and analysis of heat transfer in composite slabs with profiled steel decking,” 2017.
[11] L. M. S. Prates, “Numerical Simulation of the Fire Behaviour of Composite Structures (Slabs) [in portuguese],” MSc thesis, Instituto Politécnico de Bragança, 2018.
[12] CEN- European Committee for Standardization, EN 1363-1: Fire resistance tests Part 1 : General Requirements, CEN-Euro. Brussels: CEN- European Committee for Standardization, 2012.
[13] CEN - European Committee for Standardization, 1365-2: Fire resistance tests for loadbearing elements - Part 2: Floors and roofs (Withdrawal), CEN-Euro. Brussels: CEN - European Committee for Standardization, 2014.
[14] Y. A. Cengel and A. J. Ghajar, *Heat and Mass Transfer: Fundamentals and Applications*. New York: McGraw-Hill Education, 2011.
[15] CEN- European Committee for Standardization, EN 1994-1-2: Design of composite steel and concrete structures. Part 1-2: General rules - Structural fire design. Brussels, 2005.
[16] CEN- European Committee for Standardization, EN 1993-1-2: Design of steel structures - Part 1-2: General rules - Structural fire design Eurocode. Brussels, 2005.
[17] CEN- European Committee for Standardization, EN 1992-1-2: Design of concrete structures - Part 1-2: General rules - Structural fire design, vol. EN 1992. Brussels, 2004.
[18] CEN- European Committee for Standardization, EN 1991-1-2, Eurocode 1: Actions on structures – Part 1-2: General actions – Actions on structures exp. to fire. Brussels, 2002.
[19] J. Jiang, A. Pintar, J.M. Weigand, J.A. Main, F. Sadek, Improved calculation method for insulation-based fire resistance of composite slabs, Fire Safety Journal – in press (2019), doi: https://doi.org/10.1016/j.firesaf.2019.02.013.
[20] CEN- European Committee for Standardization, EN 1994-1-1: Design of composite steel and concrete structures - Part 1-1: General rules and rules for buildings. Brussels, 2004.